Solid state transformations from spheres to polyhedra in hollow Fe spheres

C. T. Guerrero

Instituto de Investigaciones en Materiales, Unidad Morelia, Universidad Nacional Autónoma de México, Campus Morelia UNAM. Antigua Carretera a Pátzcuaro No. 8701, Col. Ex-Hacienda de San José de la Huerta, 58190, Morelia, Michoacán, México,
e-mail: centli.guerrero@iim.unam.mx

I. A. Figueroa

Instituto de Investigaciones en Materiales, Universidad Nacional Autónoma de México, Circuito Exterior S/N, Cd. Universitaria, 04510, Ciudad de México, México.

J. A. Verduzco

Instituto de Investigación en Metalurgia y Materiales, Universidad Michoacana de San Nicolás de Hidalgo, Edificio U, Ciudad Universitaria, 58030, Morelia, Michoacán, México.

L. Pérez

Department of Mechanical Engineering, Universidad Técnica Federico Santa María, Av. España 1680, Casilla 110-V, Valparaíso, Chile.

L. Bejar

Facultad de Ingeniería Mecánica, Universidad Michoacana de San Nicolás de Hidalgo, Edificio W, Ciudad Universitaria, 58000, Morelia, Michoacán, México.

O. Hernández

Escuela Nacional de Estudios Superiores, Unidad Morelia, Universidad Nacional Autónoma de México, Campus Morelia UNAM, Antigua Carretera a Pátzcuaro No. 8701, Col. Ex-Hacienda de San José de la Huerta, Morelia, Michoacán, 58190, México.

I. Alfonso

Instituto de Investigaciones en Materiales, Unidad Morelia, Universidad Nacional Autónoma de México, Campus Morelia UNAM, Antigua Carretera a Pátzcuaro No. 8701, Col. Ex-Hacienda de San José de la Huerta, 58190, Morelia, Michoacán, México.

Received 9 December 2022; accepted 1 March 2023

The present work analyzes the sintering conditions for $\sim$ 3 mm inner diameter hollow iron spheres, sintered for manufacturing composite structures. Optimal sintering variables were investigated modifying temperature from 700 to 1200°C, while times were between 1 and 3 h. Results showed that packing of the spheres increased with time and temperature: at 700°C sintering was not enough; at temperatures from 800° to 1000°C spheres were well sintered with porosity between them; while at higher temperatures were completely packed. Densities ranged from 0.6 gcm^{-3} to a maximum of 1.1 gcm^{-3} for spheres 100% packed, where it was observed a sphere-to-polyhedron shape transformation, with maximum values of penetration (0.39 mm) and sintering neck width (1.42 mm). Complete packing of the Fe particles of the sphere walls was also observed. The use of Design of Experiments made possible to establish correlations between sintering variables and characteristics such as neck width, penetration, porosity and packing. These results could be used as a starting point for the adequate selection of the sintering conditions of hollow Fe spheres for manufacturing hollow composite structures, taking into account not only the characteristics of the sintered hollow spheres but also of the Fe particles forming their walls.

Keywords: Composite structures; syntactic foams; hollow spheres; sintering.

DOI: https://doi.org/10.31349/RevMexFis.69.051001

1. Introduction

The importance of the cellular metals has increased in the last decades motivated by their applications, such as transportation industry structural parts, filters, energy absorbers and heat exchangers, as show the works of Banhart [1] and Zhu *et al*. [2] .These applications are possible due to their low density and a combination of mechanical, thermal, acoustic, chemical and electrical properties. Among the types of cellular metals are the metallic foams, which can be classified into conventional and syntactic. Conventional metallic foams consist of a metal structure with pores, which can be interconnected or not, being their low density the most characteristic property [1]. On the other hand, syntactic foams, also known

as Metal Matrix Syntactic Foams (MMSFs), have closed pore cells, and are formed by porous reinforcements or fillers. This kind of foams is used when high mechanical properties are required since the hollow spheres not only decrease density but also act as reinforcements. This leads to higher stiffness and compressive strength than conventional foams. Some of their applications are in marine equipment, sandwich parts in composite materials, and structural components in the aerospace industry [3–8]. Their properties depend on the characteristics of the microspheres, such as relative quantities spheres/metal, material of the spheres and wall thickness. Among the reported reinforcements are hollow spheres of different materials, mainly metals or ceramics, embedded in a matrix, being aluminum alloys the most used [8, 9]. Hollow spheres can be used not only for manufacturing syntactic foam but as part of Metal Hollow Sphere Structures (MHSS). Among the types of MHSS are lose spheres, sintered structure, adhesive bonded or brazed structure, and cast structure, used by Göhler *et al*. [10]. This last classification includes metal foams. The hollow iron spheres (HIS) are one of the most studied reinforcements for manufacturing these materials, as demonstrated the works of Rabie *et al*. [6, 7]. They are mainly produced by powder metallurgy by the process developed by Jaeckel in 1987, patented by Jaeckel and Smigilski [11], consisting in coating Fe particles and a binder suspension in a fluidized bed, followed by a heat treatment where the green-spheres are transformed into solid hollow sphere shells by sintering. Manufacturing the metallic hollow spheres by sintering occurs when powder particles are heated up to about 80% of their melting temperature [12]. This allows to obtain hollow spheres with reproducible structures regarding to dimensional tolerance, density, and mechanical behavior. Among other methods, MMSFs can be manufactured mixing hollow microspheres with metallic powders or infiltrating a molten metal into the microspheres. Examples are the works of Szlancsik *et al*. [3], who studied the compressive behavior and microstructural characteristics of iron hollow spheres reinforcing an aluminum matrix; or Xue *et al*. [13], who manufactured and characterized Ti matrix syntactic foams. One of the processes reported in literature for infiltration consists on packing the hollow spheres into different devices, which include ceramic or metallic grids to avoid the movement between the spheres and achieve a homogenous infiltration, successfully used by Orbulov and Dobránszky [14]. Also using infiltration, Rabiei and O'Neill [6] had a better control of the packing, reporting a range of spheres volume inside the matrix from 30 to a maximum of approximately 62%. It is important to remark that the space between the spheres (porosity) will correspond to the volume of the infiltrated metal. It is reported that packing can be controlled modifying variables as the infiltration pressure, or avoiding the movement of the spheres through their sintering in a first step to obtain a preform and then infiltrate the molten metal through it [14, 15]. Sintering is known as the process to bond powders or particles and create defined raw or green compacts, heating in a controlled atmosphere, at a temperature below the melting point of the particles, but high enough to allow the individual particles to bind at their surfaces. Sintering occurs when materials are exposed to high temperatures during specific time since occurs atomic diffusin and consolidation as well as re arrangement in loosely packed bodies. During sintering, the particles diffuse across the boundaries of the grain, fusing the particles together and creating one solid piece. Sintering phenomenon involves fusion of particles, volume reduction, decrease in porosity and increase in grain size [16]. The ideal sintering temperature is 0.5 Tm (melting temperature) and a time as long as necessary. For metals in solid solution, the sintering temperature is $2/3$ - $3/4$ Tm, therefore the temperature and the residence time are related to the composition, the surface state and the properties required by the product. For the particular case of Fe, sintering takes place at 1000-1200°C [17–19]. The permanence time is short if the sintering occurs at high temperatures and it is longer if it is at low temperatures, although in practice sintering time is determined by experimentation. Generally, low sintering temperature and short duration time are preferred. According to the above commented, if the hollow spheres are sintered in a first step, their sintering level can modify the porosity between them and hence the quantity of metal which fills these pores. Packing plays an important role in the final mechanical properties of sintered MHSS, which also depend on the relative quantities matrix-hollow spheres. Sintering leads to materials with more uniform and predictable properties, as showed Rabiei *et al*. [7], but its disadvantage is the strict control of the sintering variables to obtain an optimum bond between the hollow spheres, which controls their packing. Insufficient temperatures or pressures could originate preforms with low green density of the spheres. Otherwise, too high temperatures could lead to excessive sintering of the spheres or to their deterioration; while pressures exceeding the compressive strength of the spheres could cause considerable damages to the preform [16]. Then, the study of the sintering process is essential, which is not only dependent on the kind of sphere but also on characteristics as diameter and wall thickness [4, 14]. As can be seen, the study of the sintered process of hollow spheres can be useful not only for manufacturing syntactic foams but also for the use of the sintered structure itself, being essential the strict control of the sintering conditions. That is why the main objective of this work is to analyze the effect of the sintering variables on the packing of Fe hollow spheres. This sintered material could be used as a part of a sintered metallic hollow sphere structures, or for their posterior use as preforms in syntactic foams manufacturing. This work also searches to find correlations between time and temperature with characteristics of the sintered structures such as sintering penetration, neck width, porosity and packing density. It is expected that adequate sintering conditions allow to obtain structures with different porosities/packings, satisfying the requirements of (i) a porous preform for manufacturing syntactic foams, or (ii) a compact hollow structure for machining complex shapes.

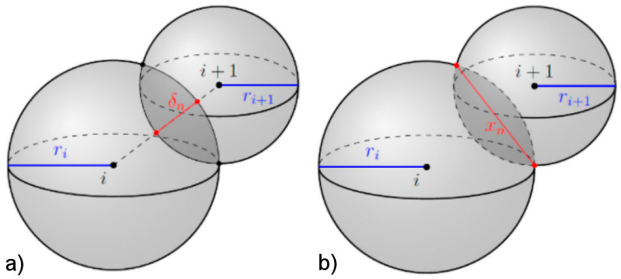

FIGURE 1. Representation of: a) penetration (δ_n) and b) sintering neck width (χ_n). r_i and $r_i + 1$ represent the radii of two neighbor spheres, i and i+1.

2. Experimental

In a first step, we received Globomet Fe hollow spheres (Hollomet GmbH, Germany) produced by powder metallurgy according to the process showed by Jaeckel and Smigilski [11], and used by Anderson *et al.* [12]. The spheres were characterized (diameter and walls) by Optical (OM) and Scanning Electron Microscopies (SEM), using respectively a Labomed Med 400 OM and a Jeol JSM IT300LV SEM operated at 20 kV. The chemical composition of the spheres was 99 % Fe, $<$ 0.2 % C, $<$ 0.2 % O, (in wt.%), with Fe as the only one phase according to the X-ray diffractometry (XRD) analysis, carried out using a Bruker D2 Phaser diffractometer with CuKα radiation ($\lambda = 1.54$ Å) at 35 kV and 25 mA. For the analysis of the sphere walls, they were mounted in epoxy resin, cut, and prepared metallographically. Once the features of the hollow spheres were stablished, they were added to the bottom of the crucible (SiC) mixed and vibrated for packing in a maximum dense arrangement to obtain reproducible results, and sintered for an initial analysis during 1 hour at temperatures ranging between 700°C and 1200°C. Sintering was carried out without applying mechanical pressure in a XINYU SA2 series furnace at vacuum of 0.08 Pa, achived with a rotary vane vacumm pump to avoid oxidation. Once the spheres sintered under these conditions were analyzed it was possible to stablish temperature ranges for obtaining porous structures (not presenting insufficient or excessive sintering). For studying the dependence of time and temperature on sintering there were produced nine preforms (for Design of Experiments, DOE), using 3 temperatures for 1, 2 and 3 h.

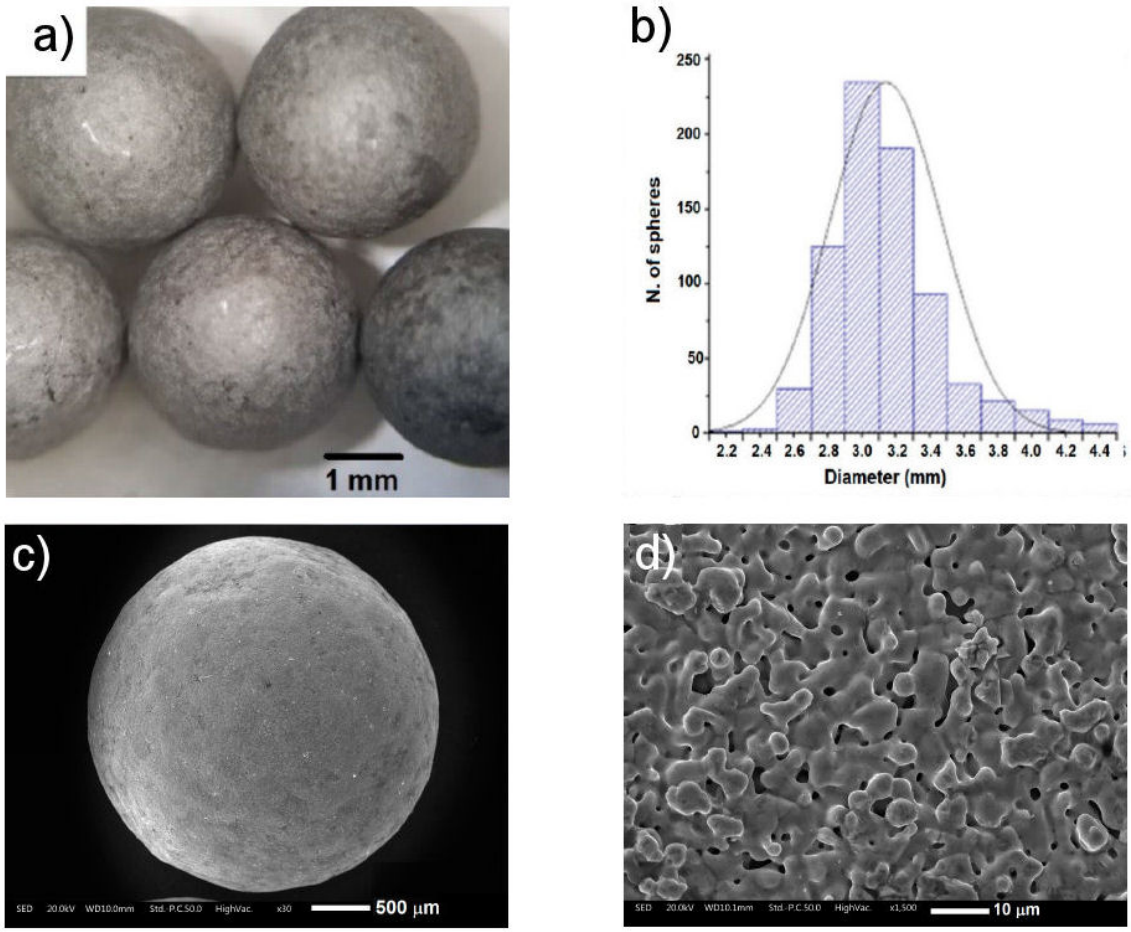

FIGURE 2. a) Macrography of the hollow Fe spheres. b) Histogram of frequencies of the hollow sphere diameter. c) SE-SEM image of a hollow sphere, and d) its surface.

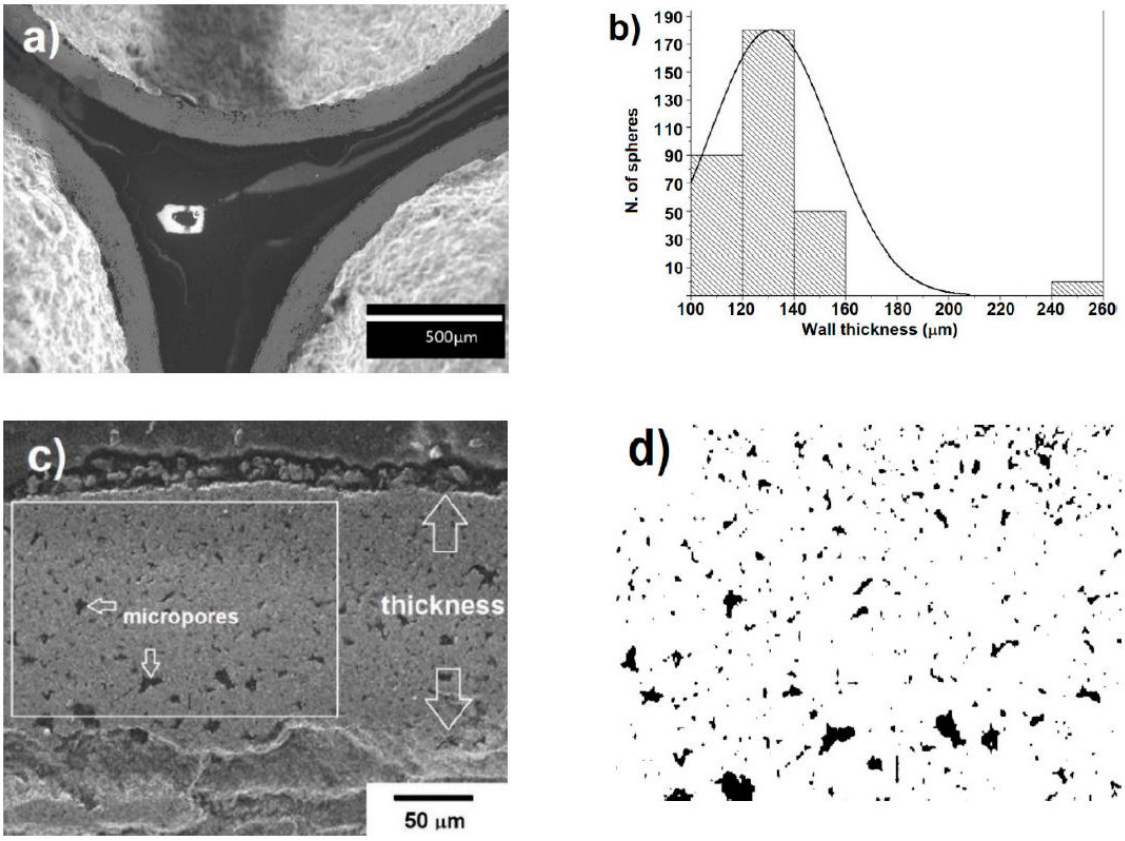

FIGURE 3. a) SE-SEM micrograph of the hollow spheres; b) frequency histogram of the wall thickness, c) amplification of the walls with microporosity; and d) modified image used for micro-porosity measurement.

After sintering the nine preforms, OM and SEM observations were performed for the analysis of the packing of the spheres and their walls. Packing (or sintered density, D) depends on the bond between spheres surfaces, and it is directly related with the resulting porosity (spaces between the spheres, P), $D = 100 - P$, in %. Sintering penetration (δ_n) and neck width (χ_n) were selected as control parameters according to the observed in Fig. 1a)-b). These parameters have been used in works such as the reported by Lu *et al*. [18], and were measured through ImageJ image analysis [19]. δ_n is the difference between the radii of two neighbor spheres before and after being sintered. Before sintering spheres are only just touching, and penetration is zero. After sintering penetration increases mainly due to the reaccommodation and shape modification of the hollow spheres.

The higher packing in the sphere walls after sintering could slightly contribute to increase penetration because the size of the spheres decreases due to the lower porosity between the Fe particles of their walls. On the other hand, χ_n is defined as the width of the join neck between two neighbor spheres, and increases due to shape modification of the hollow spheres. δ_n and χ_n are parameters that depend on temperature and time, leading to different adhesion between particles. Before sintering the spheres are barely in contact, almost only by one point, while after sintering spherical shape is lost and neck formation occurs. For a better statistical analysis, 10 images were obtained from different zones for each sphere-sphere bonding.

Porosity was also measured through image analysis. It is expected the increase of D, δ_n and χ_n, and the decrease of P with the increase in temperature and time. The correlations of sintering time t and temperature T with these characteristics of the sintered structures were established using multifactorial n^k DOE and the support of Statgraphics Centurion XV software [20]. The number of experiments used in this design was $N = n^k = 3^2 = 9$, where n is the quantity of conditions ($n = 3$; 3 temperatures and 3 different times) and k the quantity of variables (k= 2, t and T). DOE has been successfully used by Ahmed *et al*. [21] for studying the relationships between porosity degree and morphology with different properties of iron metal compacts.

3. Results and discussion

The characterization of the Fe hollow spheres showed that their average diameter was 3 ± 0.3 mm. This is observed in Fig. 2a), which shows the shape and size of the spheres. As can be seen the diameter is variable, more precisely detailed in Fig. 2b), where the frequency histogram of the diameter is shown. This histogram reveals that the diameters range from 2.6 to 4.6 mm, distribution which agrees well with the

reported in literature for these spheres [4, 6, 12]. Figure 2c) shows a SE-SEM (secondary electrons) image of a hollow sphere, while Fig. 2d) presents a micrography of its surface, where it can be seen the microstructure composed by sintered Fe particles of ~ 3 μm, with sintering necks between them. Microporosity between particles is clearly observed, which will be further analyzed.

Figure 3a) shows a SE-SEM image of sectioned spheres where there are observed their walls, while the frequency histogram of the wall thickness is depicted in Fig. 3b). As can be noted, thickness is irregular, being the average 130 ± 10 μm. This leads to a diameter/wall thickness ratio of 23, like the reported for similar spheres by Rabiei *et al*. [7] and by Garcia-Avila and Rabiei [4]. The wall porosity originated in the manufacturing process of the spheres can be observed in more detail in Fig. 3c). Porosity for the rectangular area of Fig. 3c) measured using ImageJ (processed image of Fig. 3d) was 13 ± 1 %, in the range of the reported in literature (between 5 and 15 %) [4,7]. According to these results, sintering density for the hollow sphere wall is 6.9 gcm^{-3}. In MHSS both macro and microporosities play important roles in the resultant mechanical properties. Macroporosity is the space between the spheres and depends on the size of the contact area of the sphere-to-sphere connection. This porosity can be open (interconnected) or closed. Otherwise, microporosity is present in the sphere walls, and as reported Friedl *et al*. [22], it can also show open porosity or be completely dense.

After the analysis of the spheres treated at temperatures from 700 to 1200°C for 1 hour it was observed that at 700°C sintering did not occur, being the spheres completely isolated and without important contact points (necks). This temperature does not fulfil the purpose of keeping the spheres together. When temperature was increased sintering of the spheres occurred, fact observed in Figs. 4a)-c), which shows respectively macrographies representing the spheres sintered at 800, 1000 and 1200°C. As temperature increases sintering is higher, as it is observed in the joint between the spheres [circled in Figs. 4a) and 4b)]. On the other hand, porosity decreases with the increase in temperature, as is clearly indicated by the reduction of spaces between spheres. At temperatures higher than 1100°C complete packing of the spheres occurs, with no spaces between them due to complete sintering and neck growth. These results show that temperatures needed for sintering the hollow spheres were similar to the used for the fabrication of hollow iron spheres, which were between 1125 and 1200°C [23]. This process can be also classified as the continuation of the sintering process of the Fe particles present in the sphere walls. The complete packing for the spheres sintered at 1200 Â°C is observed in Fig. 4c), and represents a problem for the use of the HIS in the manufacturing of syntactic foams because there are not spaces for the introduction of metal powders or a molten metal (infiltration). Nevertheless, spheres sintered during 1h at 1100 or 1200°C could be used for obtaining compact machinable sintered structures. Lower temperatures could also be applied for this purpose, but under the risk of debonding of the spheres during machining. Densities of the sphere sintered structures ranged from 0.6 gcm^{-3} obtained at 800°C, to 1.1 gcm^{-3} obtained at 1200°C. The strength of the sintered hollow spheres highly depends on the contact areas between them: when there are small contact areas the spheres are weakly bonded together and the structure shows poor mechanical properties. Under these conditions failures follow the contact areas between the spheres, leaving the spheres mostly intact. Otherwise, for higher contact areas the mechanical properties are improved because the spheres are strongly bonded together, the material thickens significantly in the contact region, and cracks are propagated through the spheres breaking them. This was reported in the works of Qi *et al*. [24], and Szyniszewski *et al*. [25]. Then, it is essential to consider the possible application of the structure, because depending on the sintering temperature the porosity will be interconnected or not. Low sintering temperatures lead to structures with interconnected porosity between the spheres, while higher temperatures could lead to the spheres deformation to polyhedral bodies due to an increase of the sintering contacts, also reducing the degree of open porosity. Besides, if the advantageous spherical shape of the spheres is modified their strength could decrease [1]. Then, for their possible use

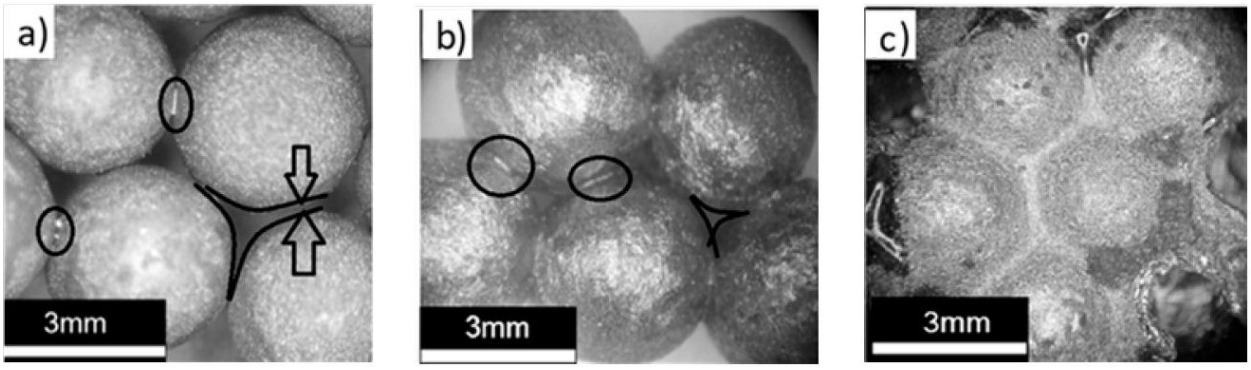

FIGURE 4. Macrographies of the spheres sintered for 1 h at: a) 800°C; b) 1000°C; and c) 1200°C.

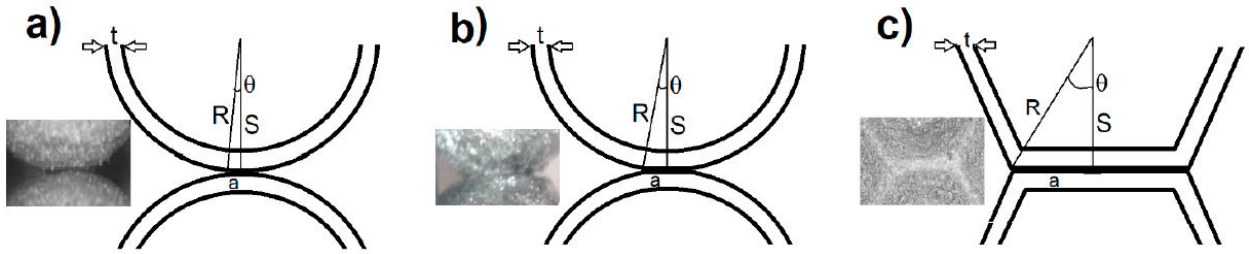

FIGURE 5. Schematic representation of the necks formation for the spheres sintered at: a) 800°C; b) 1000°C; and c) 1200°C.

as preforms in manufacturing syntactic foams by infiltration temperatures must be controlled between 800 and 1000°C. That is why temperatures of 800, 900 and 1000°C and times of 1, 2 and 3 h were selected for analyzing the effect of sintering conditions on the spheres packing.

As it was observed in Figs. 4a) to c), with the increase in the sintering temperature the contact areas between the spheres increased: from small contact areas in Fig. 4a) with the spherical shape of the spheres intact, to a completely compact structure in Fig. 4c) where spheres lost their spherical shape and hexagons can be assumed. This complete packing obtained at high temperatures leads to a sphere-to-polyhedron shape transformation. The curvature of the neck almost disappears, and the spheres are flattened on the bonded contact area, which agrees the reported by Veyhl *et al*. [26]. This sphere-to-polyhedron shape transformation and the subsequent decrease in porosity was found by Bjørk *et al*. [27] during the analysis of the sintering behavior of close-packed spheres, reporting the final shapes as tetrakaidecahedra. The modification of the bonded areas (flattened) is schematically represented in Figs. 5a)-c), trying to reproduce the observed in Figs. 4a)-c). These approximations agree with the work of Fallet *et al*. [28], who modelled the contacts between sintered hollow spheres. As it can be seen, a relationship can be stablished between the radius (R) of a completely spherical sphere (which also is the maximum radius of the formed hexagon), the minimum radius (S) of a sintered sphere (which is the minimum radius or apothem of the formed hexagon), and the half of the sintering neck width (a).

$$\sin\theta = \frac{a}{R}. \tag{1}$$

Assuming that wall thickness (t) remains constant, the value of penetration is:

$$\delta = 2(R - S), \tag{2}$$

where δ increases with the increase of the neck width value. Maximum value of neck width (χ) is achieved for the hexagon shown in Fig. 5c), being 1.57 mm. This is calculated assuming that during sintering without applying pressure volume remains constant and the perimeters of the circle and the hexagon are the same (9.42 mm according to the radius of the spheres $R = 1.5$ mm). Maximum penetration for this value of sintering neck width is δ = 0.44 mm, being δ =0 for the spheres barely in contact depicted in Fig. 5a). These values agree well with maxima experimental penetration (0.39 mm) and sintering neck width (1.42 mm), obtained for spheres completely packed observed in Fig. 4c). Experimental values slightly lower than the theoretically expected could be attributed to the increase in the packing of the Fe particles of the sphere walls, which reduces the volume of the hollow spheres.

Once the analysis of the effect of temperature was carried out and selected the DOE for the study of the alloys, it is necessary a more in deep study of the contact between spheres. Figures 6a)-i) show SEM images of spheres sintered at different combinations of times and temperatures for the analysis of: i) packing and porosity (left), ii) sintering neck width (center), and iii) sintering of the Fe particles through the study at higher magnifications of the bonding area between neighbor spheres (right). As it can be seen in Figs. 6a), 6d) and 6g) in all cases sintering between the sphere surfaces is present, bonding their walls and increasing the penetration and the formation of necks. It is clearly observed that packing increases with the increase in time and temperature, decreasing the spaces between the spheres (porosity). Figures 6b), 6e) and 6h) show that neck longitude clearly increases with the increase in sintering time and temperature, decreasing its curvature, which agrees with the already observed in Figs. 5a)-c). Otherwise, packing of Fe particles also increased with the increase in time and temperature, as it is observed in Fig. 6c), 6f) and 6i), decreasing the porosity between Fe particles. It is important to remark that this was the continuation of the sintering process for the already sintered Fe particles (sintered in the process to form the spheres). This can lead to a significant increase in density, reducing pores and improving mechanical properties, which depend on the fraction, size, distribution and morphology of the porosity [29]. This phenomenon was observed for the spheres sintered at 800 during 1 h (see Fig. 6c), where the porosity in their walls decreased to values 6% (sintering density of 7.43 gcm^{-3}). Comparing this image with Fig. 2d), where there were observed sintered Fe particles of $\sim$ 3 μm with sintering necks, it can be noted that for sintering at 800°C during 1h individual Fe particles are difficult to identify due to their bonding, with few sintering necks still observed. The increase in sintering time and temperature led to the improvement in the formation of necks and the development of polyhedric grains, as it can be observed in Figs. 6f) and 6i), which agrees with the reported by Davari *et al*., [23]. These grains

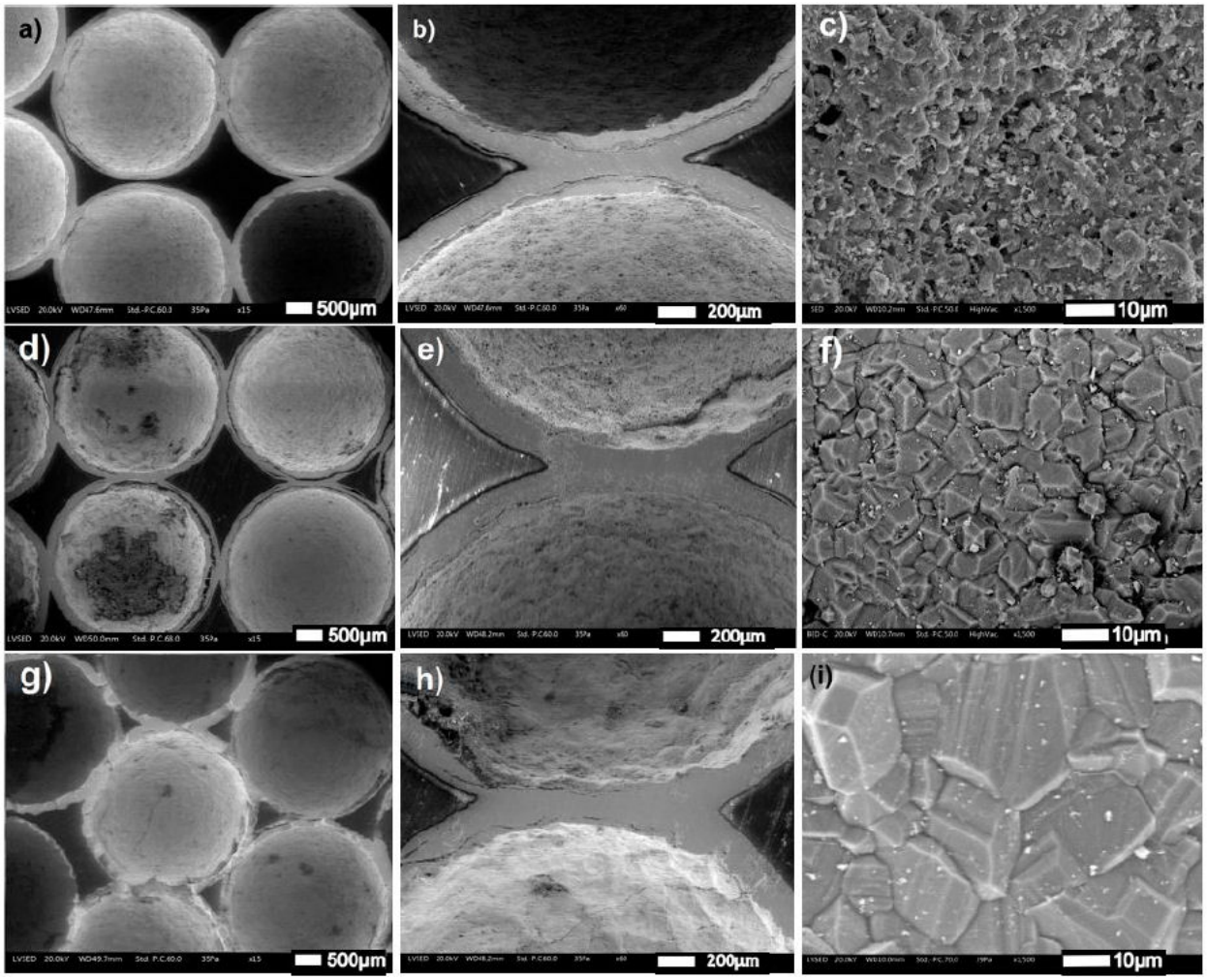

FIGURE 6. SEM micrographs of spheres and their walls for different sintering conditions: 800°C for 1 h a)-c), 900°C for 2h d)-f) and 1000°C for 3h g)-i).

are completely consolidated and packed, showing well-defined boundaries and perfect junctions, without intergranular pores. Davari *et al*. [23] studied the sintering process to produce hollow Fe spheres, and reported that increasing both the temperature and the sintering time the atoms had more time to diffuse to the contact point's areas, leading to decline shells porosity. The grain size increased from ~ 10 μm for the spheres sintered at 900°C for 2 h, to ~ 25 μm for the spheres sintered at 1000°C for 3 h, which indicates the final stage of sintering. Complete packing and grain formation led to this shape transformation, where particles transformed in polyhedra (tetrakaidecahedra) [27]. Due to the irregular shapes of the Fe particles in this case the sphere-to-polyhedron did not result in exact hexagons, as it was observed for the hollow spheres in Fig. 4c). Besides, surfaces in Figs. 6f) and 6i) are smoother compared to the porous sintered structures of the spheres sintered at 800°C for 1 h [Fig. 6c)] and for the spheres before sintering [Fig. 2d)]. These modifications are part of the three stages of sintering. Initial stage can be observed for the as received hollow spheres in Fig. 2d), being reported rearrangement of particles and necking. At the intermediate stage grain boundaries are formed, growing the size of the necks, and decreasing porosity because the particles move closer. The final stage of sintering shows rigid crystal structure with few isolated pores, and grains with hexagonal structure, as found in their works Low *et al*. [30] and Azis *et al*. [31]. It is also important to remark that a too high sintering temperature could result in degradation of properties if grain growth exceeds a critical size, also increasing wall microporosity [29, 32]. Over-heating or over-burning was reported by Hu *et al*. [33] for the sintering of different Fe powders, decreasing density and mechanical properties due to the reduction of the bonding strength between grains. Figures 6f) and 6i) show that although the grains grew the particles remained completely consolidated, without porosity. In the present research the effect of sintering on the mechanical properties of the spheres will not be studied, but it is reported that a higher sintering density due to a higher bonding area leads to the increment of the mechanical strength. Hollow spheres with dense sintered cell walls have higher ductility and strength compared to

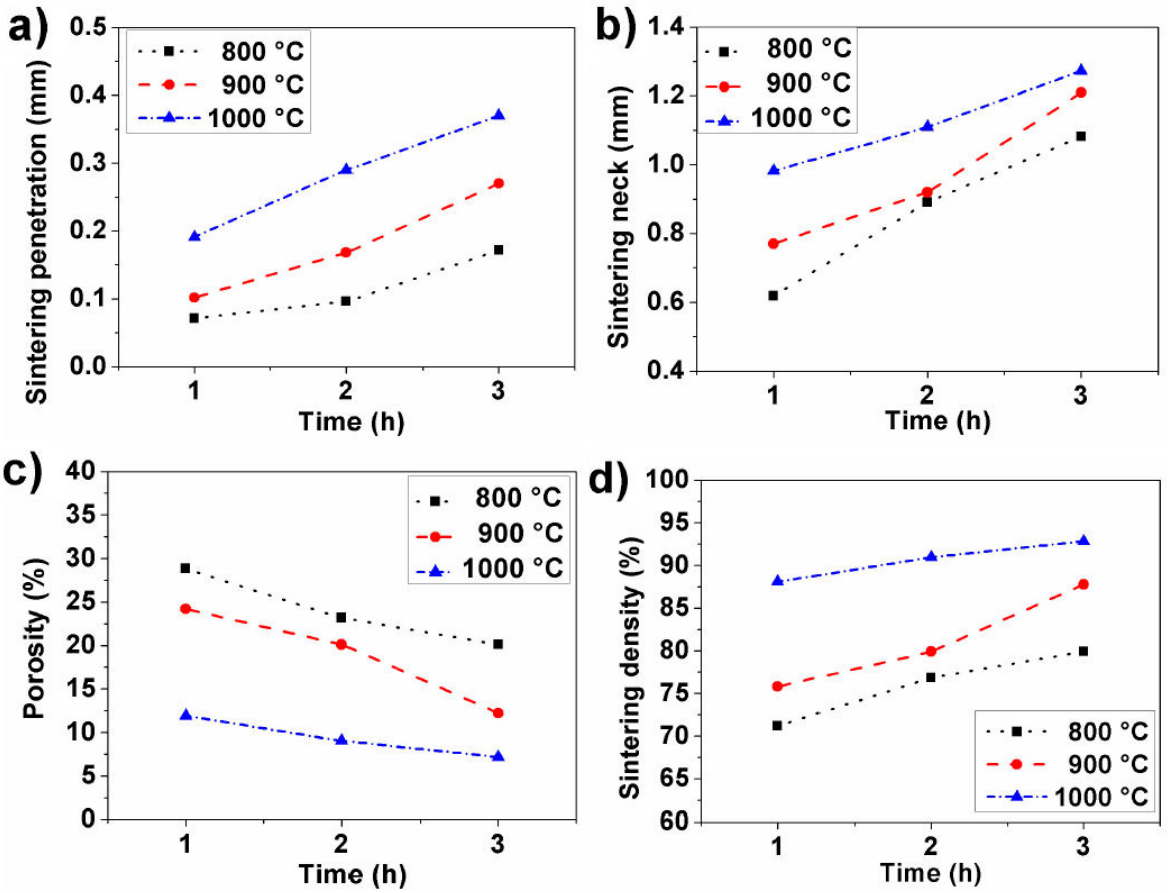

FIGURE 7. Averages for sintering penetration a), neck width b), porosity c) and packing d), for spheres sintered at different times and temperatures.

hollow spheres with porous walls [22]. This aspect could be an extra variable for the study of the mechanical behavior of MHSS, being important both macro and micro porosities. Besides, for syntactic metal foams the strength of the preform is directly related with the strength of the foam.

Figures 7a)-c) show the results obtained for sintering penetration, neck width and porosity at 800, 900 and 1000°C for times of 1, 2 and 3 h. This was calculated using image analysis of the SEM images. It can be observed that for the three different times the tendence is that the increase in temperature leads to the increase in sintering neck width [Fig. 7a)] and penetration [Fig. 7b)], decreasing porosity [Fig. 7c)] due to the increase in packing density [Fig. 7d)]. This behavior is also observed for the increase in sintering time at a same temperature, and it is attributed to the densification of the spheres due to their sintering, which is favored by time and temperature. As can be seen, maxima values for penetration and sintering neck width were obtained for the hollow spheres sintered at 1000°C during 3 h, being 0.37 and 1.27 mm, respectively, lower than experimental maxima and theoretical calculations using Figs. 5a)-c), which were $\chi = 1.57$ mm and $\delta = 0.44$ mm. Otherwise, minimum porosity and maximum packing density were 7.17 and 92.83 %, respectively, also obtained for high temperatures and long times. An excessive porosity reduction is undesirable to produce foams by infiltration since permeability of the molten alloy decreases. Nevertheless, if an enough fluidity of the molten metal is reached a low porosity could be important for the increase of the final density of the syntactic foam, needing a higher quantity of reinforcing hollow spheres and a lower quantity of metal matrix. Minimum packing density in Fig. 7d) is close to 72%, which is comparable with the maximum theoretical packing density of spherical particles ($\phi_{\max} \approx 0.74$), but higher than the typical packing densities ($\phi \approx 0.64$), reported by Veyhl *et al.* [26]. Its increase to values higher than 90 % can be attributed to the plastic deformation and accommodation of the spheres.

Figures 8a)-d) show, for the selected DOE, the response surface curves for the effect of sintering times and temperatures on penetration, neck width, porosity and packing, obtained using Statgraphics Centurion XV [20]. As can be seen, spheres sintered at higher temperatures and for longer times have the higher values of penetration [Fig. 8a), in red] and neck width [Fig. 8b), in red], therefore obtaining lower porosity in comparison to those spheres sintered at lower temperatures and for shorter times [Fig. 8c), in blue]. In addition, Fig. 8d) shows that the highest values of packing are obtained at high temperatures and long times (in red). The Pareto's

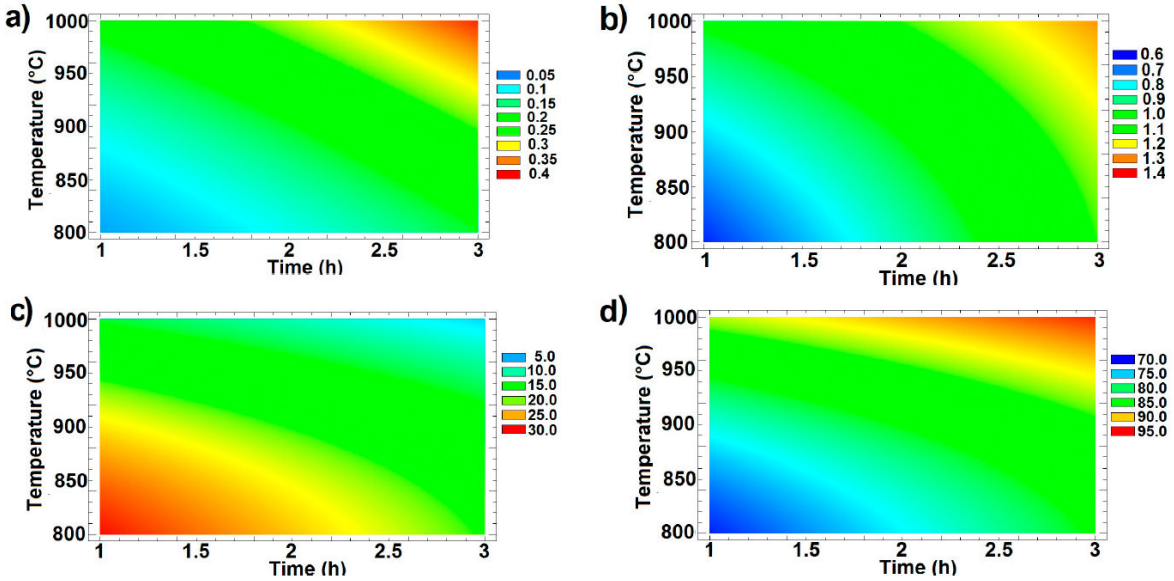

FIGURE 8. Response surfaces obtained using DOE and Statgraphics Centurion XV for the effect of time and temperature on: a) penetration, b) neck width, c) porosity and d) packing.

Anova analysis showed that both variables (t and T) significantly affect sintering, although temperature had a more important effect.

The results obtained using DOE allowed to establish the following dependences between time t and temperature T with penetration δ, neck width χ, porosity P and packing density D, with R^2 in all the cases higher than 0.9:

$$\delta = 1.136 - 0.146t - 0.003T + 0.011t^2 + 0.0002tT + 0.00000183T^2, \quad (3)$$

$$\chi = 0.725 + 0.521t - 0.002T + 0.015t^2 - 0.0004tT + 0.0000025T^2, \quad (4)$$

$$P = -62.481 - 13.085t + 0.293T - 0.038t^2 + 0.01tT - 0.0002143T^2, \quad (5)$$

$$D = 162.481 + 13.085t - 0.293T + 0.038t^2 - 0.01tT + 0.0002143T^2. \quad (6)$$

This allowed to obtained estimations with relative errors lower than 10%, showing that DOE could be an effective tool for controlling the characteristics of preforms and hollow structures manufactured by hollow spheres sintering. This through the choose of the adequate input variables during the sintering process.

4. Conclusions

After the analysis of the effect of time and temperature on the packing of sintered hollow iron spheres, the following can be concluded:

- Temperatures for obtaining adequate sintering, with the presence of porosity between the spheres, ranged between 800 and 1000°C. At temperatures lower than 800°C sintering did not occur, while at temperatures higher than 1100°C the hollow spheres were completely packed, without porosity between them.
- Image analysis showed that sintering penetration, neck width and density (packing) significantly increased with the increase in time and temperature. Maxima sintering penetration (0.39 mm) and neck width (1.42 mm) were obtained when the spheres were 100 % packed, with flattened necks, which led to transform the hollow spheres in polyhedra with hexagonal shapes in the contact areas of the sphere-to-sphere connection.
- Sintering density of the Fe particles forming the sphere walls increased with the increase in time and temperature, with the development of grains which grew and were completely packed, presenting polyhedral structures. This led to decrease almost to zero the porosity in the sphere walls.
- Density of the sintered spheres increased from 0.6 gcm^{-3} to a maximum of 1.1 gcm^{-3} for spheres completely packed, while density of the sphere walls increased from 6.9 gcm^{-3} for the as-received spheres to 7.9 gcm^{-3} for the hollow spheres with walls presenting polyhedral structures.
- The use of Design of Experiments (DOE) allowed to obtained correlations between time and temperature and characteristics of the hollow spheres such as penetration, neck width, porosity and packing. This also allowed to conclude that temperature was the most important variable affecting sintering.

- This study is including not only the characteristics of the sintered hollow spheres but also of the Fe particles forming their walls, and it could serve as a starting point for the adequate selection of the sintering conditions of hollow Fe spheres depending on the desired application of the resulting hollow structure.

Acknowledgements

Authors acknowledges the financial support from PASPA DGAPA-UNAM and SEP CONACYT 285215 project. The participation of Departamento de Ingeniería de Procesos e Hidráulica, Universidad Autónoma Metropolitana-Iztapalapa is also acknowledged. This work was also supported by UNAM-PAPIIT IN102322 project.

1. J. Banhart, Manufacture, characterisation and application of cellular metals and metal foams, *Progress in Materials Science* **46** (2001) 559, https://doi.org/10.1016/S0079-6425(00)00002-5.
2. C. Zhu *et al*., Fabrication and optimization of combined open-and-closed-type cellular metals, *Materials Design (1980-2015)* **56** (2014) 291, https://doi.org/10.1016/j.matdes.2013.11.018.
3. A. Szlancsik *et al.*, Compressive Behavior and Microstructural Characteristics of Iron Hollow Sphere Filled Aluminum Matrix Syntactic Foams, *Materials* **8** (2015) 7926, https://doi.org/10.3390/ma8115432.
4. M. Garcia-Avila and A. Rabiei, Effect of Sphere Properties on Microstructure and Mechanical Performance of Cast Composite Metal Foams, *Metals* **5** (2015) 822, https://doi.org/10.3390/met5020822.
5. L. Licitra *et al.*, Dynamic properties of alumina hollow particle filled aluminum alloy A356 matrix syntactic foams, *Materials Design* **66** (2015) 504, https://doi.org/10.1016/j.matdes.2014.03.041.
6. A. Rabiei and A. O'Neill, A study on processing of a composite metal foam via casting, *Materials Science and Engineering: A* **404** (2005) 159, https://doi.org/10.1016/j.msea.2005.05.089.
7. A. Rabiei *et al*., Processing and Characterization of a New Composite Metal Foam, *Materials transactions* **47** (2006) 2148, https://doi.org/10.2320/matertrans.47.2148.
8. A. Rabiei and L. Vendra, A comparison of composite metal foam's properties and other comparable metal foams, *Materials Letters* **63** (2009) 533, https://doi.org/10.1016/j.matlet.2008.11.002.
9. M. Altenaiji *et al.*, Characterisation of aluminium matrix syntactic foams under drop weight impact, *Materials Design* **59** (2014) 296, https://doi.org/10.1016/j.matdes.2014.03.002.
10. H. Goehler *et al*., Metallic hollow sphere structures - Status and outlook in Proceedings of the Conference on Cellular Materials (CELLMAT-2012, Dresden, Germany).
11. M. Jaeckel and H. Smigilski, Coating of polymeric spheres with particles (European Patent DE3724156, 1988).
12. O. Andersen *et al.*, Properties and applictions of low-cost hollow sphere structures, *Processing and Fabrication of Advanced Materials* **VIII** (2001) 59, https://doi.org/10.1142/9789812811431_0007.
13. X. bing XUE *et al*., Manufacturing, compressive behaviour and elastic modulus of Ti matrix syntactic foam fabricated by powder metallurgy, *Transactions of Nonferrous Metals Society of China* **22** (2012) s188, https://doi.org/10.1016/S1003-6326(12)61707-5.
14. I. Norbert Orbulov and J. Dobránszky, Producing metal matrix syntactic foams by pressure infiltration, *Periodica Polytechnica Mechanical Engineering* **52** (2008) 35-42, https://doi.org/10.3311/pp.me.2008-1.06.
15. I. N. Orbulov and K. Májlinger, Description of the compressive response of metal matrix syntactic foams, *Materials Design* **49** (2013) 1, https://doi.org/10.1016/j.matdes.2013.02.007.
16. R. Njoku and A. Kennedy, Effects of sintering temperature on the density and porosity of sodium chloride preforms for open celled aluminium foam manufacturing, *Nigerian Journal of Technology* **32** (2013) 117, https://doi.org/10.4314/njt.321.615.
17. N. Gupta and P. Rohatgi, Metal matrix syntactic foams: Processing, microstructure, properties and applications (DEStech Publications Inc., 2014).
18. N. Dukhan, Metal foams: fundamentals and applications (DEStech Publications, Inc, 2013).
19. N. Dukhan, *Metal Foams: Fundamentals and Applications* (DEStech Publications, Incorporated, 2013), https://books.google.com.mx/books?id=xZRG1EyBbzsC.
20. J. Lu *et al.*, Role of interconnections in porous bioceramics on bone re- colonization in vitro and in vivo, *Journal of Materials Science: Materials in Medicine* **10** (1999) 111, https://doi.org/10.1023/A:1008973120918.
21. W. Rasband, ImageJ, https://imagej.nih.gov/ij.
22. Statgraphics, Centurion XV Version, https://www.statgraphics.com/.
23. Y. M. Z. Ahmed *et al*., Mechanical properties and porosity relationship of porous iron compacts, *Powder Metallurgy* **52** (2009) 72, https://doi.org/10.1179/174329008X315584.
24. O. Friedl *et al.*, Experimental investigation of mechanical properties of metallic hollow sphere structures, *Metallurgical and Materials Transactions B* **39** (2008) 135. https://doi.org/10.1007/s11663-007-9098-2.

25. H. R. Davari *et al.*, Effect of sintering parameters (time and temperature) upon the fabrication process of organic binder-based metallic hollow sphere, *Powder Metallurgy* **60** (2017) 363, https://doi.org/10.1080/00325899.2017.1355424.

26. F. Qi *et al*., A novel way to prepare hollow sphere ceramics, *Journal of the American Ceramic Society* **97** (2014) 3341.

27. S. Szyniszewski *et al.*, The mechanical properties and modeling of a sintered hollow sphere steel foam, *Materials & Design (1980-2015)* **54** (2014) 1083. https://doi.org/10.1016/j.matdes.2013.08.045.

28. C. Veyhl *et al*., Thermal conductivity computations of sintered hollow sphere structures, *Metals* **2** (2012) 113, https://doi.org/10.3390/met2020113.

29. R. Bjørk *et al*., The sintering behavior of close-packed spheres, *Scripta Materialia* **67** (2012) 81, https://doi.org/10.1016/j.scriptamat.2012.03.024.

30. A. Fallet, *et al*., Discrete element simulation on the behaviour of random hollow sphere metal foams, In European International Powder Metallurgy Congress and Exhibition 2008 (European Powder Metallurgy Association (EPMA), 2008) pp. 189-194.

31. N. Chawla and X. Deng, Microstructure and mechanical behavior of porous sintered steels, *Materials Science and Engineering: A* **390** (2005) 98, https://doi.org/10.1016/j.msea.2004.08.046.

32. M. Liu, Sintering Technology (IntechOpen, Rijeka, 2018), https://doi.org/10.5772/intechopen.75146.

33. A. Muthuchamy *et al*., An investigation on effect of heating mode and temperature on sintering of Fe-P alloys, *Materials Characterization* **114** (2016) 122, https://doi.org/10.1016/j.matchar.2016.02.015.

34. J. L. H. H. Youhua Hu, Yimin Li and X. Zhang, Effects of Sintering Temperature and Holding Time on Densification and Mechanical Properties of MIM HK30 Stainless Steel, *International Journal of Metallurgy and Metal Physics* **3** (2018), https://doi.org/10.35840/2631-5076/9222.

35. Z. H. Low, I. Ismail, and K. S. Tan, Sintering Processing of Complex Magnetic Ceramic Oxides: A Comparison Between Sintering of Bottom-Up Approach Synthesis and Mechanochemical Process of Top-Down Approach Synthesis, In M. Liu, ed., Sintering Technology, chap. 2 (IntechOpen, Rijeka, 2018), https://doi.org/10.5772/intechopen.78654.

36. N. Dukhan, Metal Foams: Fundamentals and Applications (DEStech Publications, Incorporated, 2013), https://books.google.com.mx/books?id=xZRG1EyBbzsC.